Kinematic Mass Model of Activated Bimolecular Reactions: Reactions of Vibrationally Excited Reactants

Marko Perdih,[†] Ian W. M. Smith,[‡] and Adolf Miklavc*[,†]

National Institute of Chemistry, Hajdrihova 19, 1001 Ljubljana, Slovenia, and School of Chemistry, The University of Birmingham, Edgbaston, Birmingham B15 2TT, U.K.

Received: June 24, 1997; In Final Form: March 5, 1998

The recently proposed simple collision model of activated bimolecular reactions, which takes into account the nonspherical shape of molecules and includes the effects of the reagent rotation, has been extended to treat reactions of vibrationally excited reagents. Vibrational excitations are supposed to affect the reaction rates primarily through changes in the position and the height of the effective barrier. Critical dividing surfaces were calculated on the assumption of vibrational adiabaticity en route to the critical dividing surface. The positions of the adiabatic barriers as well as their heights were found to depend significantly on the choice of coordinates and the definition of the reaction path. Two approaches were considered. The analysis which gave thresholds in closest agreement with the values from quasiclassical trajectory (QCT) calculations, and which was therefore adopted in the present calculations, uses a local mode analysis along the reaction path expressed in terms of internal coordinates. Reaction cross sections were calculated for a range of translational energies for O + HCl($v = 1$), O + DCl($v = 1$), and O + H_2($v = 1$). The results were compared with those for vibrationally unexcited reagents and both of these sets of model results were further compared with the cross sections from QCT calculations. It was evident that one significant difference between model and QCT results arises because the model only estimates "forward flux" through the chosen critical dividing surface, whereas trajectories allow for the possibility of "recrossing", thus lowering the reactive flux. Transmission factors allowing for this effect were calculated. The corrected model results are in satisfactory agreement with the QCT results although some discrepancies remain. Possible reasons for these remaining differences are discussed.

I. Introduction

Simple collision models of bimolecular reactions retain their importance in chemical reaction dynamics, despite great advances in experimental and computational methods. Comparison of their predictions with experimental results, or with the results from more sophisticated scattering calculations, can provide considerable insight into the dynamics of reactive collisions. In efforts to rationalize particular features of experimental data or the results of complex calculations simple models can be very helpful. Furthermore, once they have been validated by comparison with accurate scattering calculations, such models, which require much less computational effort than accurate calculations, might be used to predict values of the rate constants outside the regimes investigated experimentally and they might be useful in the modeling of processes involving complex chemical species.

In simple models of chemical reactions, attention is focused on the reacting system at the "critical dividing surface"[1] separating reactants from products. Reaction is assumed to occur if the relevant component of the kinetic energy exceeds the effective potential energy on this surface. The original line-of-centers (LOC) model[2−4] was derived using this assumption, as was the subsequent extension of it, now generally referred to as the angle-dependent-line-of-centers (ADLOC) model.[1,5−9] This model has been later modified and developed[10−18] on the basis of the same energy considerations as in the original formulation.

More recently, by defining a "kinematic mass" for the collisions between reagents, the requirement for total angular momentum conservation, which restricts the amount of kinetic energy available for barrier crossing, was built into simple models.[18−20] The effects of rotational excitation of the reactants could be taken into account[19,20] while preserving the essential simplicity of the treatment. Effects of vibrational zero-point energy could also be included in a simple way,[20] by determining the effective barrier heights on the assumption of vibrational adiabaticity en route to the barrier.

In the present paper we extended the model proposed in refs 19 and 20 to treat reactions of atoms (A) with vibrationally excited ($v = 1$) diatomic molecules (BC). There is considerable current interest in the effects of reagent vibrational excitation on the rates of bimolecular reactions both of the simplest type, A + BC, and of those which involve polyatomic reagents.[21] The observed effects can often be rationalized in terms of vibrationally adiabatic transition state theory (VA-TST),[22,23] which assumes vibrational adiabaticity in the progress of the system from large reagent separation up to the position of the maximum on the appropriate vibrationally adiabatic potential energy curve. The assumption of vibrational adiabaticity has been tested for vibrationally excited reagents against classical trajectories in ref 24. Furthermore, it has been tested at thermal

* To whom correspondence should be addressed.
[†] National Institute of Chemistry.
[‡] The University of Birmingham.

S1089-5639(97)02413-4 CCC: $15.00
Published on Web 05/13/1998

TABLE 1: The Position and Height of the Barrier for the Collinear F + H_2(v = 0, 1, 2) Reaction As Determined by the Present LNM(α) and LNM(γ) Methods and by the Periodic Orbit Dividing Surface (pods) Method in Ref 29

	LNM(α)			LNM(γ)			pods		
v	r_1 (Å)	r_2 (Å)	E_b (kcal/mol)	r_1 (Å)	r_2 (Å)	E_b (kcal/mol)	r_1 (Å)	r_2 (Å)	E_b (kcal/mol)
0	0.749	1.740	0.585	0.750	1.697	0.698	0.746	1.745	0.576
1	0.744	2.015	0.283	0.745	1.896	0.398	0.746	2.111	0.254
2	0.743	2.197	0.181	0.743	2.043	0.278	0.735	2.412	0.323

energies in calculations which combined transition state theory with quasiclassical trajectories (QCT).[25] It was demonstrated in ref 25 that, at the energies in question, the adiabatic assumption was valid to a high degree of approximation for both exothermic reactions, with "early" barriers, and for thermoneutral reactions, with barriers placed approximately midway along the minimum energy path leading from reagents to products. The assumption of vibrational adiabaticity has also been tested for vibrationally excited reagents against accurate quantum dynamics.[26]

The vibrationally adiabatic potentials $V_{ad}(s,v)$ used in VA-TST comprise two terms:

$$V_{ad}(s,v) = V(s) + E_{vib}(s,v) \tag{1}$$

the electronic potential energy $V(s)$, which only depends on the position s along the reaction path, and $E_{vib}(s,v)$, which is the energy of the v-th quantum state associated with the vibrational motion orthogonal to the reaction path which transforms in the limit $s \rightarrow -\infty$ into the BC vibration. In general, whereas the zero-point energy correction (i.e., $E_{vib}(s,v=0)$) mainly changes the effective height of the adiabatic energy barrier but the changes of its position are usually small, both the position and the height of the barriers are changed by vibrational effects when $v \geq 1$[22,23] (Table 1). In the present work, we have based our definitions of the critical dividing surfaces for A + BC(v = 1) reactions on the concepts used in VA-TST which we have just outlined. Examples of how the size and the shape of the critical dividing surface are changed when the reagent is vibrationally excited are given in Figure 1.

However, it is important to appreciate that the size and shape of the critical dividing surface and the effective energy barriers on this surface depend on what is assumed about the reaction coordinate. We adopted the "local normal mode" (LNM) picture, as promoted, e.g., in the paper of Agmon,[27] but the reaction path chosen here is different from those considered by Agmon. In the present work the reaction path is defined to be along one of the local normal modes, hereafter referred to, somewhat inexactly, as the "asymmetric mode". The local separability of the motions parallel and perpendicular to the path is then assumed. In view of the simplicity of our model the effects of the bending mode have been neglected. It will be clear that the reaction path chosen here satisfies the two conditions derived by Natanson[28] which uniquely determine the internal intrinsic path as he has defined it. The most essential property which marks out the internal intrinsic path is that the slow motion along the path is separated from the vibrations. The internal intrinsic path can generally coincide with a gradient following path only in collinear collisions.[28a] The model was formulated either in the internal coordinates (r_1, r_2, α) or in the coordinates (r, R, γ), where $r = r_1 = r_{BC}$, $r_2 = r_{AB}$, $\alpha = \pi - \angle$(C − B − A), and (R, γ) are the usual Jacobi coordinates.

The thresholds predicted using these two definitions of the reaction path were compared with those from QCT calculations and with the, presumably more accurate, barriers obtained by periodic orbit analysis.[29] The agreement was better when the internal coordinates (r_1, r_2, α), i.e., LNM(α), were used and they were adopted in subsequent calculations. With this model we calculated the kinetic energy dependence of the total cross section for the reactions O + HCl (v = 1), O + DCl(v = 1), and O + H_2(v = 1), with the reactants in the rotational ground state (j = 0), and compared the predictions of the model with the QCT calculations.[30,31] The choice of the rotational state ensures that there are no "rotational shadowing effects" of the kind described earlier.[20] Furthermore, the above examples were chosen because our previous studies[20] involving reactants in v = 0 showed that effects associated with the deflection of trajectories from straight line paths prior to their reaching the critical dividing surface appeared to be rather small in these systems.

II. The Kinematic Mass Model

Simple models of activated bimolecular reactions have been founded on the assumption that en route to the barrier reactive trajectories can be adequately approximated by straight line trajectories. A collision is supposed to be reactive if the system has enough energy to overcome the barrier. In any model, the energy available to overcome the barrier must be determined, as well as the shape of the critical dividing surface and the barrier height.

Energy Available To Overcome the Barrier. For the sake of completeness we present here a brief derivation of the energy available to overcome the barrier within the kinematic mass model[19,20] for diatomic molecules reacting with atoms. The parameters used in the model are defined in Figure 2. At each point of the trajectory the conserved total angular momentum $\mathbf{J}_0$ is given by

$$\mathbf{J}_0 = \mathbf{j} + \mu\mathbf{R} \times \mathbf{v} = \mathbf{j} + \mu\mathbf{R} \times \mathbf{v}_n + \mu\mathbf{R} \times \mathbf{v}_{II} \tag{2}$$

where $\mathbf{j}$ is the rotational angular momentum of the molecule, μ is the reduced mass of the collision partners, $\mathbf{v}$ is the relative translation velocity, $\mathbf{v}_n$ is the component of velocity in the direction normal to the potential energy surface, $\mathbf{n}$, shown in Figure 2, $\mathbf{v}_{II}$ is the component of the velocity parallel to the surface, and $\mathbf{R}$ is the vector from the center of mass of the molecule to the atom (see Figure 2). It is convenient to write

$$\mathbf{J}_0 = \mathbf{J} + \mu\mathbf{R} \times \mathbf{v}_{II} \tag{3}$$

where

$$\mathbf{J} = \mathbf{j} + \mu\mathbf{R} \times \mathbf{v}_n = \mathbf{j} + \mu v_n \mathbf{R} \times \mathbf{n} \tag{4}$$

The sum of the translational and rotational energies E_k can be then written as:

$$E_k = \frac{1}{2}\mu\mathbf{v}^2 + \frac{\mathbf{j}^2}{2I} = \frac{1}{2}\mu\mathbf{v}_n^2 + \frac{1}{2}\mu\mathbf{v}_{II}^2 + \frac{\mathbf{j}^2}{2I} \tag{5}$$

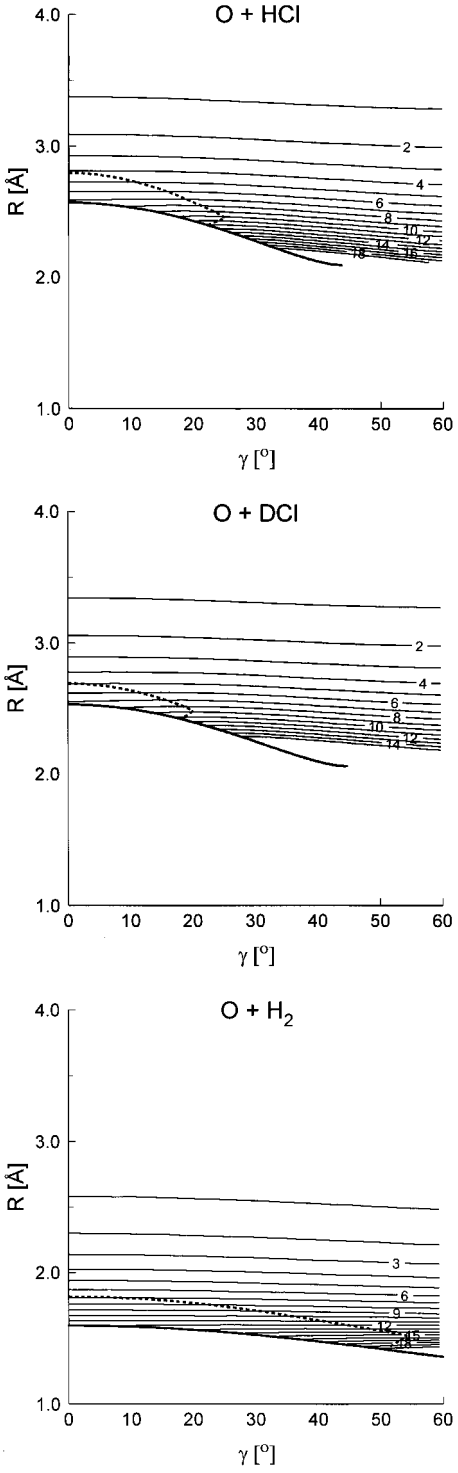

Figure 1. The shape of the critical dividing surfaces for $v = 0$ and $v = 1$, and the equipotential curves calculated at the relaxed interatomic distances of the diatomic for the reactions O + HCl, O + DCl, and O + H_2, on the corresponding potential energy surfaces.[30,31] The shapes of the critical dividing surfaces are calculated using the LNM(α) approach (see text for details). The numbers on the contours correspond to the potential energy in kcal/mol relative to the reactants. The solid curve represents the critical dividing surface for $v = 0$, and the dashed curve represents the critical dividing surface for $v = 1$. At a certain value of α the position of the vibrationally adiabatic barrier is shifted abruptly to the region of the electronic barrier. This instability leads to the double values when the transformation to Jacobi coordinates is made.

where I is the moment of inertia of the molecule. Equation 5 can be recast in the following form:

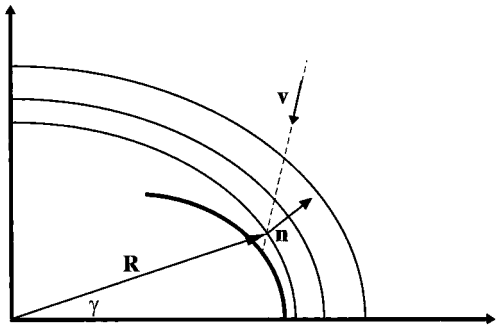

Figure 2. Schematic representation of a molecule-atom collision. The heavy line represents a part of the critical dividing surface; lighter lines are equipotential contours calculated with the reactant in the relaxed geometry. **v** is the relative velocity of the collision partners, **R** is their center of mass separation, **n** is the normal to the equipotential energy surface, and γ is the Jacobi angle. Straight line trajectories up to the critical dividing surface are assumed. **v**, **n**, and the axis of BC need not to be in the same plane.

$$E_k = \frac{1}{2}\mu v_{II}^2 + \frac{1}{2}\mu^* v^{*2} + \frac{\mathbf{J}^2}{I + \mu(\mathbf{R} \times \mathbf{n})^2} \tag{6}$$

where

$$\mu^* = \frac{\mu}{1 + \dfrac{\mu(\mathbf{R} \times \mathbf{n})^2}{I}} \tag{7}$$

and

$$v^* = v_n - \frac{\mathbf{j}\cdot(\mathbf{R} \times \mathbf{n})}{I} \tag{8}$$

Equation 6 for the total kinetic energy E_k is valid at any point on the trajectory. If the reaction occurs in a sudden regime, it may be assumed that it is controlled by the motion over a small element dS of the potential energy surface near the barrier. Vectors **R**, **n** and $\mathbf{v}_{||}$ may be assumed not to change much during the motion on dS. Consequently, the first and the third term in eq 6 for E_k must be regarded as nearly constant on dS, whereas the second term can undergo large changes. It is therefore the energy given by this term that is available to overcome the barrier. In other words, the reaction may be assumed to occur if the following condition is fulfilled:

$$\frac{1}{2}\mu^* v^{*2} \geq E_b \tag{9}$$

where E_b is the barrier energy at the point of the critical dividing surface lying on the line of the trajectory. It should be noted that $\mu^*/\mu \leq 1$ and that the deviation of this ratio from unity reflects the importance of rotational recoil in the system. v^*, on the other hand, can greatly exceed v_n, depending on the rotational velocity.

The condition for a collision to lead to te reaction expressed in eq 9 will cause the reaction cross sections predicted by the present model to differ from those of the ADLOC model[1,5−9] and extensions of the model.[10−18] Nevertheless, for direct activated bimolecular reactions, which all of these models are designed to treat, the reaction cross section is expected to rise monotonically with translational and rotational energy from the energetic threshold.

Shape of the Critical Dividing Surface and the Barrier Height. We turn here to the problem of determining the shape of the critical dividing surface and the barrier height. Our

analysis is based on the assumption of vibrational adiabaticity and is limited initially to the potential energy surfaces for collinear reactions. The treatment is then extended to noncollinear encounters. The assumption of separability of the motion parallel and transverse to the reaction coordinate is essential for defining the frequency for the transverse motion. The vibrationally adiabatic potential $V_{ad}(s,v)$ at any point s along the reaction path was given in eq 1.

To satisfy the above requirements the internal intrinsic path as defined by Natanson[28] was chosen here because it has the essential property that the slow motion along the path is separated approximately from the vibrations. We note again that the gradient-following path can generally coincide with the internal intrinsic path only for collinear collisions.[28a] In determining the path we found the local normal mode approach[27] to be quite helpful. The essence of the normal mode approach is in simultaneous diagonalization of the kinetic and potential energy matrices. This ensures that the motion along the normal modes is separable. It is customary to perform this analysis for motion in a potential well or at a potential saddle point—in both cases the first derivatives vanish. As pointed out in ref 27, this fact is irrelevant as far as local separability is concerned because first derivatives, upon changing the coordinates, transform to a linear combination of the first derivatives in the new coordinates. Calculations of normal modes and frequencies can thus be performed at any point on a potential surface, provided we neglect terms higher than second order in the expansion of the potential. What one obtains by this analysis are "local normal modes" (LNM) and their separability is "local". Globally they are coupled because of the higher order terms in the expansion of the potential, and also dynamically, through the dependence on the configuration.

The matrix **F** of the quadratic form in the power expansion of the potential function has to be determined as a function of coordinates chosen, and also the matrix **G** of momentum coupling. Because we are neglecting the bending mode, **F** and **G** are just 2×2 matrixes.

To obtain the internal intrinsic reaction path, the points were determined at which

$$\frac{\partial V}{\partial Q_s} = 0 \tag{10}$$

where Q_s is the symmetric local normal mode. At such points the conditions (1) and (2) from ref 28b are satisfied which uniquely determine the reaction path. The asymmetric local vibrational mode Q_a coincides then with the gradient of the potential in the local (Q_s, Q_a) coordinate system. At each point the reaction coordinate points along the local asymmetric vibrational mode and hence the local separability assumption holds. The idea of minimizing the energy in a direction transverse to the reaction coordinate is actually an old one,[28c] although the implementations of it differ somewhat.

The above reaction coordinate has been proposed already,[27] but so far it has apparently not been tested in any calculations. Furthermore, the method of calculation[27] starting from the saddle point and following the direction of the local mode Q_a could be less stable, because of numerical difficulties. The condition that each point of the reaction coordinate must be at the center of the local symmetric mode can be more easily implemented numerically.

The procedure outlined above can be implemented rigorously in dealing with a collinear atom-transfer reaction A + BC → AB + C. With $r_1 = r_{BC}$ and $r_2 = r_{AB}$, the kinetic energy is given by[27]

$$T = \frac{1}{2}(\mu_1 \dot{r}_1^2 + \mu_2 \dot{r}_2^2 + 2m_A m_C \dot{r}_1 \dot{r}_2 / M) \tag{11}$$

where m_A, m_B, and m_C are the masses of the atoms, $M = m_A + m_B + m_C$ is the total mass, μ_1 and μ_2 are the reduced masses for relative translation in reactants and products, respectively

$$\mu_1 = m_A(m_B + m_C)/M \tag{12}$$

$$\mu_2 = m_C(m_A + m_B)/M$$

The dots denote the time-derivatives. The two-dimensional kinetic energy matrix $\mathbf{T}^r$ has then the elements: $T_{11}{}^r = \mu_2$, $T_{22}{}^r = \mu_1$, $T_{12}{}^r = T_{21}{}^r = m_A m_C/M$. The superscript r denotes the choice of (r_1,r_2) coordinates. In the same coordinate system the force constant matrix $\mathbf{F}^r$ can be defined: $F_{11}{}^r = \partial^2 V/\partial r_1{}^2$, $F_{22}{}^r = \partial^2 V/\partial r_2{}^2$, $F_{12}{}^r = F_{21}{}^r = \partial^2 V/\partial r_1 \partial r_2$. Because $\mathbf{T}^r$ is positive definite, one can find a new basis (Q_s, Q_a) in which $\mathbf{T}^Q$ is the unit matrix and $\mathbf{F}^Q$ is diagonal. It is because (Q_s, Q_a) generally depend on configuration that they are called "local normal mode" coordinates. In an infinitesimal neighborhood of any point (r_1, r_2) the motion is separable in the $(Q_s(r_1,r_2), Q_a(r_1,r_2))$ coordinate system, provided that the potential is approximated by a Taylor expansion up to the second-order terms.

In determining LNM coordinates the standard procedures[32] can be followed. One first finds the vibrational frequencies ω_i associated with them, as eigenvalues of $\mathbf{F}^r$ in a space with the metric tensor $\mathbf{T}^r$

$$\mathbf{F}^r Q = \omega^2 \mathbf{T}^r Q \tag{13}$$

Nontrivial solutions of eq 13 exist provided ω is one of the roots of the characteristic equation

$$\det(\mathbf{F}^r - \omega^2 \mathbf{T}^r) = 0 \tag{14}$$

ω^2 is real, because $\mathbf{T}^r$ is symmetric and positive definite. The corresponding eigenvectors (local normal modes) Q_s and Q_a are found by solving the linear equations (13).

The barrier for a noncollinear collision may in the present model be evaluated for fixed values of the bending angle (α or γ). We shall use the adiabatic scheme as proposed in ref 33. Because the vibrational motion is the fastest, we may freeze the bending−rotational motion in the calculation of the barrier as a function of bend angle. The ensuing problem is similar to that in the collinear case, in the sense that for a fixed value of the bend angle the vibrational problem involves only two degrees of freedom. The local normal-mode analysis was performed by the method described in ref 32. For the O + HCl reaction the $v = 0$ and $v = 1$ vibrationally adiabatic barriers were also calculated with full normal-mode analysis. The results differ only slightly from those obtained by the above simplified approach.

III. Results of Calculations

With the model described above we calculated the kinetic energy dependence of the total cross sections for the reactions O + HCl($v = 1$), O + DCl($v = 1$), and O + H_2($v = 1$) with the reactants in their rotational ground state ($j = 0$), and compared the predictions of the model with the QCT calculations. Our previous work[20] on these reactions with reactants

in $v = 0$ showed that the effects precluding the applicability of the model are small in these cases.

The adiabatic barriers, as pointed out in the preceding section, depend on the definition of the reaction coordinate. We have therefore considered two plausible approaches to the barrier calculation: the path along the asymmetric local normal mode in Jacobi coordinates (LNM(γ)) and the path along the asymmetric local normal modes in internal coordinates (LNM(α)). LNM(α) is the internal intrinsic reaction path as defined by Natanson.[28] The adopted method of normal-mode analysis (ref 32) assumes that at each point mass-skewed, mass-scaled coordinates are used. Because the potential is approximated by the expansions up to the second-order terms the results of the two approaches may generally differ.

The barriers obtained by the reaction paths considered for the collinear geometry are shown in Figure 3 where the corresponding thresholds estimated from the QCT results are also given, for comparison. We see that the barrier height, as well as its position, depend on the definition of the reaction coordinate. The potential surface for $F + H_2$ reaction used in the QCT calculations is oblate in the relevant barrier region which precludes the application of simple models[20] based on the straight line trajectories. This is due to the strong reorientation effects occurring on such surfaces. Therefore, in this case, the barrier could not be used for model calculations of cross sections. We studied it because in this system the adiabatic barrier evaluated with the periodic orbits method[29] is also available for comparison, in addition to the QCT results. The adiabatic barriers for reaction $F + H_2(v = 0, 1, 2)$ obtained by application of the LNM(α) and LNM(γ) are presented in Table 1 with those found by calculating periodic orbits on the same potential energy surface.[29] Results from the LNM(α) method are in closer agreement with those found using periodic orbit analysis.

From Figure 3 we see that the approach in which local normal modes in internal coordinates (i.e., LNM(α)) are used to define the reaction path also gives collinear vibrationally adiabatic barriers that are generally in good agreement with the threshold energies derived from QCT calculations. Although we recognize that these two quantities are not actually the same because of "nonadiabatic leakage" in the trajectories, these effects are generally small.[25] Consequently, and because we wish to compare our present results with those from QCT calculations in the absence of accurate quantum scattering results for the systems that we have studied, we have based our calculations on the reaction paths given by the LNM(α) method. Once the values of (r_1, r_2, α) at the critical dividing surface were established, they were transformed into the Jacobi coordinates (r, R, γ) for use in the model. The γ-dependence of the bare electronic potentials and of the vibrationally adiabatic potentials for $v = 0$ and 1 is shown in Figure 4.

The reactions $O(^3P) + HCl(DCl) \rightarrow OH(OD) + Cl$ ($\Delta H_0° =$ 0.95 kcal/mol) are examples of nearly thermoneutral heavy + light-heavy systems. We have used the prolate potential surface (Surface I) for which the QCT results were reported in ref 30. For HCl($v = 1$), the threshold estimated from the QCT calculations is slightly more than 2 kcal/mol, which is in good agreement with the LNM(α) reaction path. The threshold obtained with the alternative reaction path definition considered here is about 3.5 kcal/mol, which is a rather poor approximation to the QCT threshold. For the isotopic reaction with DCl($v =$ 1), the differences in the vibrationally adiabatic maxima obtained by the different reaction paths are not as large as those for HCl;

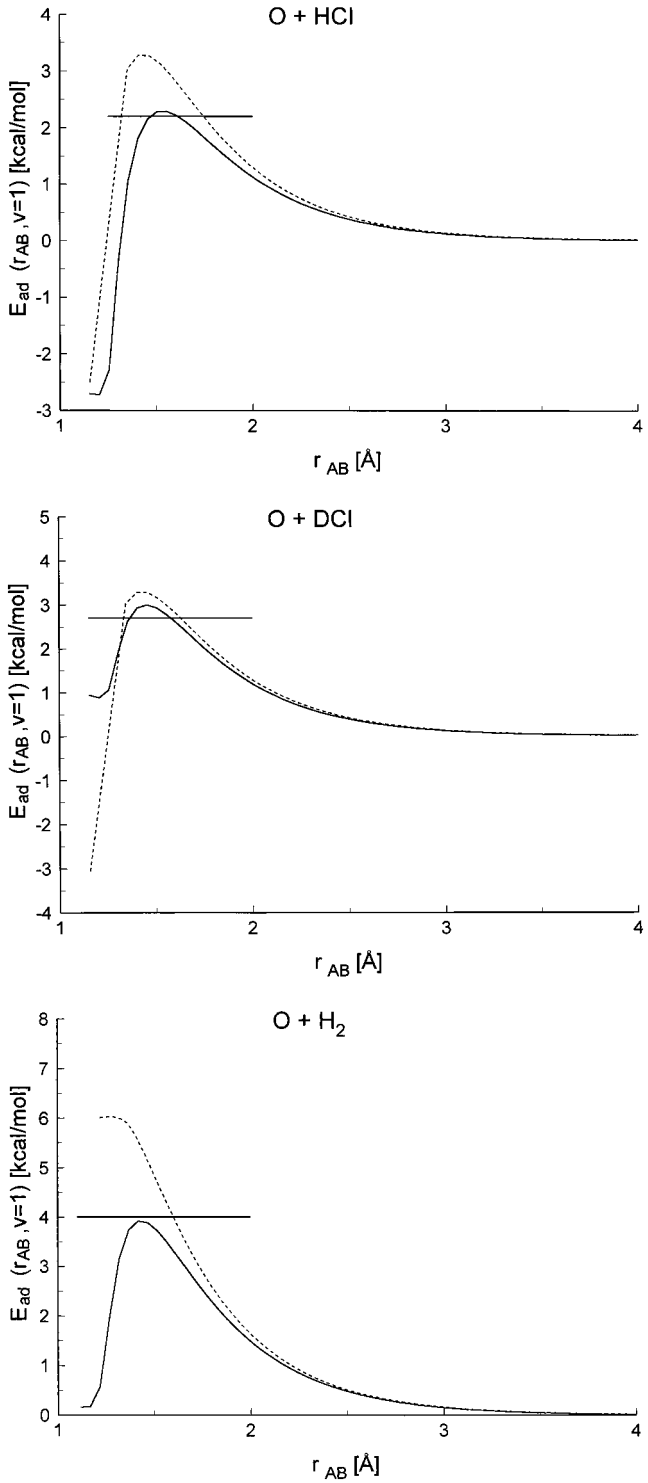

Figure 3. The dependence of the vibrationally adiabatic energy on r_{AB} (A = O, B = H,D) for the collinear geometry of reactions calculated by the two approaches defined in the text: LNM(α) (—), LNM(γ) (- - -). The full horizontal lines indicate the threshold energies for reactions estimated from QCT calculations.[30,31]

the LNM(α) path, however, still gives the best agreement with the threshold from the QCT calculations.

Although the QCT results which were already published[30] could be used to choose the method of calculation of the vibrationally adiabatic barrier, we found it necessary to redo the QCT calculations of the kinetic energy dependence of the cross section. There were several reasons for this. The cross sections in ref 30 were calculated at a rotational temperature of 300 K and it was found that rotational numbers up to $j = 8$

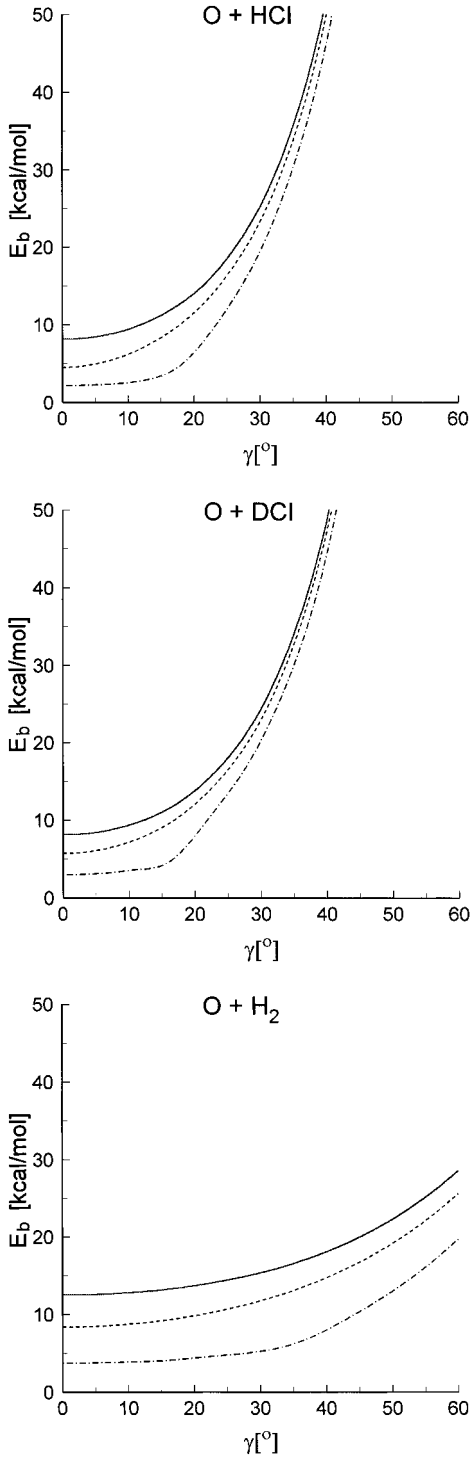

Figure 4. The dependence of the barrier height on the angle γ: (—) pure electronic barrier; (- - -) vibrationally adiabatic barrier for $v = 0$; (—•—•) vibrationally adiabatic barrier for $v = 1$.

contributed appreciably to the thermally averaged cross sections. To exclude any possible effects of rotational shadowing[20] (these will be studied in more detail in a separate paper) we performed QCT calculations for $j = 0$. Furthermore, 5000 trajectories were used here for each cross section calculation, to improve the statistics.

Finally, performing QCT calculations allowed us to examine the extent of "recrossing" which occurs in these systems in full-scale trajectories. Recrossing occurs when a trajectory having first passed through a surface in coordinate space defined to separate reagents from products in the direction reagents → products, subsequently passes through the same dividing surface in the direction products → reagents. An odd number of such crossings leads to reaction, whereas an even number does not. As in transition state theory,[34] the present model only calculates the total forward flux through the critical dividing surface and makes no allowance for subsequent recrossings, which lower the cross section or rate constant for reaction.

Therefore, to be able to compare the model and the QCT results properly, the extent of recrossing had to be determined, because this result had not been reported previously for the reactions in question. The surface separating reagents from products was chosen to be that defined by the position of the barrier in (R,γ) coordinate system. The recrossing properties of a number of trajectories were investigated also by using the separating surface defined by $r_1/r_2 = r_{1,e}/r_{2,e}$, where $r_{1,e}$ and $r_{2,e}$ are the equilibrium internuclear distances in the reagent and product molecules. The results of the two approaches were in agreement with the trajectories investigated. Energy and vibrational state dependence of the transmission factors $\kappa = N_{\text{react}}/(N_{\text{react}} + N_{\text{recross}})$, where N_i is the number of trajectories in a sample leading to the specified result, were calculated for O + HCl($v = 0$, 1) and O + DCl($v = 0$, 1) and are shown in Figure 5. There are no major differences between the recrossing properties in these two reactions. As expected for heavy + light-heavy systems, the extent of recrossing is rather large.

For $v = 0$, values with κ close to 0.8 are found at kinetic energies below 6 kcal/mol. κ then decreases with increasing kinetic energy, reaching a value of ca. 0.43 at 12 kcal/mol collision energy. The cross sections determined in our earlier work (ref 20, Figures 12 and 13) should be corrected for recrossing over the energy region $E_{\text{tr}} > 7$ kcal/mol. However, this will not change the overall picture qualitatively. For $v = 1$, κ does not differ much from the value 0.4 over the entire kinetic energy range.

In Figures 6 and 7 the dependence of the reaction cross section S_r on translational energy calculated with the present model, with and without corrections for recrossing, is compared with that found from our QCT calculations for O + HCl($v = 0$, 1) and O + DCl($v = 0$, 1). Corrections due to recrossing are made by calculating $S_r = \kappa S_r^\circ$, where S_r° is the cross section given by the model assuming no recrossing. The agreement between the model and the QCT results is very good for $v = 0$. For $v = 1$ the model cross sections are smaller than those for QCT at all energies, but the agreement can still be regarded as satisfactory, considering the simplicity of the model. Possible reasons for the disagreement between the model results with recrossing included and the QCT results for O(^{3}P) + HCl, DCl($v = 1$) are discussed below.

The reaction O(^{3}P) + H_2 → OH + H ($\Delta H_0^\circ = 2.0$ kcal/mol) is a slightly endothermic heavy + light-light reaction. The potential energy surface and the QCT results, to which we refer, are presented in ref 31. From the results in Figure 3 we see that both the position and the height of the barrier depend even more strongly than in the cases of O + HCl(DCl) on the definition of the reaction path. For LNM(α), the barrier maximum for collinear O + H_2($v = 1$) is about 4 kcal/mol, which is in good agreement with the QCT threshold. It is slightly displaced into the entrance channel. The barrier maxima calculated with the other definition of the reaction coordinate is higher and less displaced. The γ-dependence of the barrier for the selected reaction path is shown in Figure 4.

Once again it was necessary to carry out QCT calculations to determine the extent of recrossing. The results of these calculations are shown in Figure 5. For both O + H_2($v = 0$)

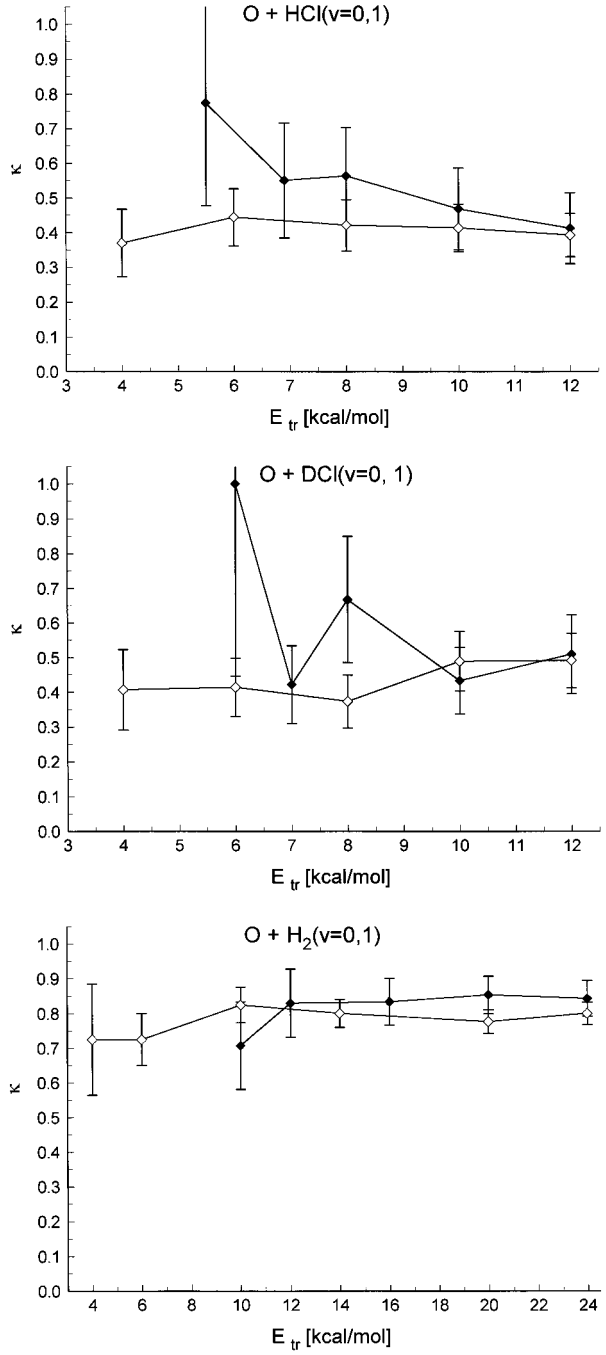

Figure 5. Translational energy and vibrational state dependence of the transmission factor κ. (◇): $v = 0$ results, (♦): $v = 1$ results, calculated at $j = 0$. The oscillations of the error arise because for increasing S_r the number of trajectories that recross ($N_{recross}$) can undergo large oscillations. It should be noted also that the total number of trajectories that cross the barrier, $N_{react} + N_{recross}$, is quite small (less than 100 out of 5000 trajectories).

and O + H_2($v = 1$), the transmission factor κ is approximately 0.8 at all values of the collision energy. This larger value, compared with those for O + HCl and O + DCl, is to be expected given the lower reduced mass of the products, in this case OH + H, which allows the products of the O + H_2 reaction to separate more quickly, thereby reducing the probability of recrossing.

The dependence of the reaction cross sections S_r on collision energy for O + H_2($v = 0$) and O + H_2($v = 1$) calculated using the LNM(α) analysis to characterize the critical dividing surface is compared with the QCT results in Figure 8. As for O + HCl and O + DCl, once allowance is made for recrossing, there is good agreement between the model and QCT results with the molecular reagent in $v = 0$. For and O+ H_2($v = 1$), the model cross sections are again uniformly smaller than those obtained in trajectory calculations.

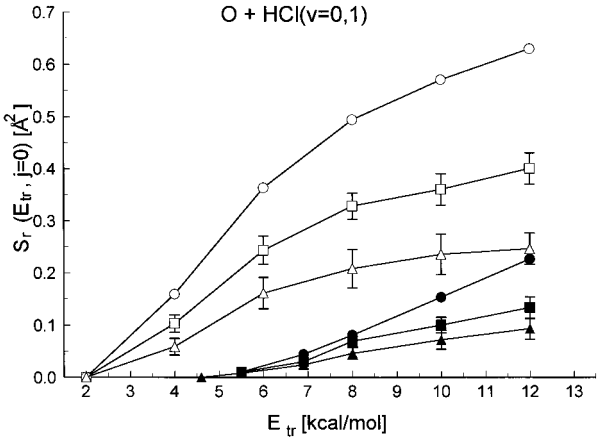

Figure 6. The dependence of the total reaction cross section S_r for the reaction O + HCl($v = 0,1$) on the translational energy E_{tr} at $j = 0$. (■, □): quasiclassical trajectory results at $v = 0$ and $v = 1$, respectively; (●, ○): model results at $v = 0$ and $v = 1$ calculated; (△, ▲): model results corrected for recrossing at $v = 0$ and $v = 1$.

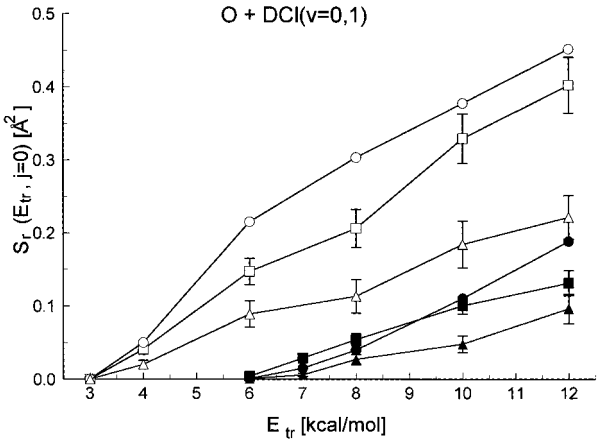

Figure 7. The same as in Figure 6 for the reaction O + DCl ($v = 0$, 1).

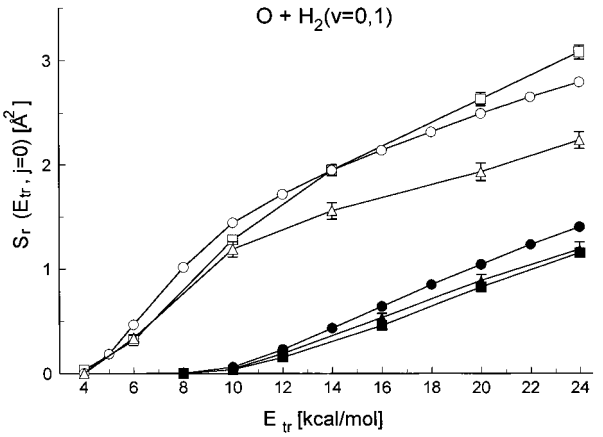

Figure 8. The same as in Figure 6 for the reaction O + H_2 ($v = 0$, 1).

IV. Discussion and Conclusions

From the present investigation we may conclude that the simple kinematic mass model[19,20] for activated bimolecular

reactions can be extended to reactions of vibrationally excited reactants provided care is taken in selecting the reaction coordinate. Both the shape of the critical dividing surface and the barrier heights on this surface depend considerably on the choice of the reaction coordinate. Effects of vibrational excitation can be modeled, similarly to vibrational zero-point energy effects,[20] on the assumption of vibrational adiabaticity en route to the barrier. The position and the height of the barrier along the path are then determined by the maximum of the vibrational adiabatic energy $V_{ad}(s,v)$.

For the four reactions considered, O + HCl(DCl), O + H_2, and F + H_2, we found that the best agreement with the thresholds estimated from the QCT results was obtained with the reaction path in internal coordinates which at each point is along the asymmetric local normal mode (LNM(α)). A symmetric local normal mode is then orthogonal to the path at each point (provided we neglect terms higher than second order in the expansion of the potential). The same approach in Jacobi coordinates (LNM(γ)) leads to barrier heights which are less satisfactory: they are generally too high, but the extent of the disagreement with the QCT thresholds is case dependent. The LNM(α) approach was therefore adapted.

As expected, the barrier heights decrease with vibrational quantum number v. Moreover, in the vicinity of the collinear geometry, the increase of the barrier height with γ is considerably slower for $v = 1$ than for $v = 0$. This leads to a larger "cone-of-acceptance" for reaction and a consequent decrease of the steric factor for reactions of vibrationally excited molecules.

The reaction cross sections predicted by the model for O + HCl, DCl($v = 0$, $j = 0$), and O + H_2($v = 0$, $j = 0$) and the dependence of these values on collision energy agree quite well with the QCT results, once allowance is made for recrossing. When the molecular reagents are in ($v = 1$, $j = 0$), and allowance is made for recrossing, the agreement becomes somewhat worse, but can still be regarded as acceptable given the simplicity of the model. The comparisons were made for reagents in $j = 0$ to avoid possible complications due to "rotational shadowing".[20]

As reported above, and in common with transition state theory,[34] the present kinematic mass model, as well as other models based on the ADLOC treatment, makes no allowance for recrossing effects. It should be appreciated that such effects are more prevalent in reactions of the heavy + light-heavy type. Therefore, in this sense and in others (see below), reactions 1 and 2 constitute particularly searching tests of the model.

The remaining discrepancy, i.e., that between predictions of QCT calculations and those of the model with corrections applied for recrossing, probably has two main origins. The first results from departures from straight line trajectories which are assumed in the model. We have already pointed out[19,20] that such effects can negate the use of the model in cases where the critical dividing surface is oblate so that full trajectories are deflected toward the region of the critical dividing surface where the barrier to reaction is low, which brings about an increase of the cross section. This is true for the F + H_2 system. So, despite the good agreement between the reaction threshold determined from QCT calculations, from the LNM(α) analysis, and from periodic orbiting dividing surfaces (PODS),[33] we have not attempted to compare the reaction cross sections from our model with those given by QCT calculations. On the prolate surfaces used in the calculations which are reported here, the effects of the intermolecular forces during the approach of the reagents to the critical dividing surface will be less, but not negligible. Furthermore, they would tend to orient the reagents unfavorably for reaction, which would lead to the QCT reaction cross sections being lower than those given by the model. However, a potential surface which is prolate at the relaxed interatomic distance r may become oblate at some other *r* values (see, e.g., ref 31(b)). Because of the intervals during which the shape of the potential energy surface is oblate the QCT reaction cross section may be higher than those given by the model in which the prolate shape of the surface at the relaxed *r* value was always assumed.

The second factor which could contribute to the discrepancy between the model cross sections and those from QCT calculations is related to the different ways in which each set of calculations is made quasiclassical. In the model, we introduce the effects of vibrational quantization at the critical dividing surface as well as at the other points of the reaction path. In QCT calculations, the initial energy in the reagent vibration is chosen to correspond to that of the vibration in the isolated molecular reagent. Although the calculations of Frost and Smith[24] showed that there is a high degree of vibrational adiabaticity as the reagents approach, the two assumptions certainly do not correspond to one another. In this regard, the reactions that we have chosen to study, i.e., O + HCl, DCl($v = 0$, $j = 0$), and O + H_2($v = 0$, $j = 0$), constitute particularly stringent tests of the model. First, because they are thermoneutral so that the barriers, at least for ($v = 0$), are located midway along the reaction path, with the result that there is a fair degree of coupling between the transverse vibration and relative translational motion en route to the barrier. Second, especially in the cases of O + HCl and O + DCl, there is a large change in the frequency of the transverse vibration as one proceeds from the separated reagents to the critical dividing surface. The QCT approach is an approximation to the exact quantum treatment and it is generally an open question to what extent the vibrational quantum level orthogonal to the reaction path is adiabatically conserved in these calculations. Because in the model calculations quantization is included, albeit approximately, at the most crucial point along the reaction path, in this respect they could be arguably superior to QCT calculations.

In conclusion, we may say that the simple kinematic mass model of activated bimolelcular reactions, developed in refs 19 and 20, can be extended to the reactions of vibrationally excited reagents. However, the accuracy of the results depends on whether one can adequately calculate the heights and positions of the vibrationally adiabatic barriers. In addition, it may be necessary to correct for recrossing effects. In the present paper, we have chosen to make this correction through full-scale QCT calculations. In practice, this is unnecessary. A computationally more efficient method would be to start trajectories on the critical dividing surface at those points and with those motions which the model predicts would lead to crossing. This method, similar to that advocated by Frost and Smith[24] in which QCT trajectories were combined with transition state theory, would then yield a value of the transmission factor, as well as the dynamic properties of the reaction products, from a relatively small number of trajectories.

Acknowledgment. Financial support of this work from the Ministry of Science and Technology of the Republic of Slovenia and the British Council is gratefully acknowledged.

References and Notes

(1) Smith, I. W. M. *Kinetics and Dynamics of Elementary Gas Reactions*; Butterworth: London, 1980.

(2) Tolman, R. C. *Statistical Mechanics with Applications for Physics and Chemistry*; Chemical Catalog Co.: New York, 1927.

(3) Frost, A. A.; Pearson, R. G. *Kinetics and Mechanism*; Wiley: New York, 1953.

(4) Present, R. D. *Proc. Natl. Acad. Sci. U.S.A.* **1955**, *41*, 415.

(5) Smith, I. W. M. *J. Chem. Educ.* **1982**, *59*, 9.

(6) Levine, R. D.; Bernstein, R. B. *Chem. Phys. Lett.* **1984**, *105*, 467.

(7) Levine, R. D. *J. Phys. Chem.* **1990**, *94*, 8872.

(8) Pelzer, H.; Wigner, E. *Z. Phys. Chem.* **1932**, *15B*, 445.

(9) Johnston, H. *Gas-Phase Reaction Rate Theory*; Ronald Press: New York, 1966.

(10) Levine, R. D.; Bernstein, R. B. *Chem. Phys. Lett.* **1986**, *132*, 11.

(11) Gislason, E. A.; Sizun, M. *J. Phys. Chem.* **1991**, *95*, 8462.

(12) Wiseman, F. L.; Rice, A. G. *J. Chem. Educ.* **1993**, *70*, 914.

(13) (a) Connor, J. N. L.; Whitehead, J. C.; Jakubetz, W. *J. Chem. Soc., Faraday Trans.* **1987**, *83*, 1703. (b) Connor, J. N. L.; Jakubetz, W. *J. Chem. Soc., Faraday Trans.* **1993**, *89*, 1481.

(14) Evans, G. T.; She, R. S. C.; Bernstein, R. B. *J. Chem. Phys.* **1985**, *82*, 2258.

(15) Evans, G. T. *J. Chem. Phys.* **1987**, *86*, 3852.

(16) Janssen, M. H. M.; Stolte, S. *J. Phys. Chem.* **1987**, *91*, 5480.

(17) She, R. S. C.; Evans, G. T.; Bernstein, R. B. *J. Chem. Phys.* **1986**, *84*, 2204.

(18) (a) Evans, G. T.; van Kleef, E.; Stolte, S. *J. Chem. Phys.* **1990**, *93*, 4878. (b) Esposito, M.; Evans, G. T. *J. Chem. Phys.* **1992**, *97*, 4846.

(19) Miklavc, A.; Perdih M.; Smith, I. W. M. *Chem. Phys. Lett.* **1995**, *241*, 415.

(20) Perdih, M.; Miklavc, A.; Smith, I. W. M. *J. Chem. Phys.* **1997**, *106*, 5478.

(21) Crim, F. F. *J. Phys. Chem.* **1996**, *100*, 12725.

(22) (a) Smith, I. W. M. In *Advances in Gas-Phase Photochemistry and Kinetics: Bimolecular Collisions*; Ashfold, M. N. R., Baggott, J. E. Eds.; RSC: London, 1989. (b) Smith, I. W. M. *Acc. Chem. Res.* **1990**, *23*, 103.

(23) (a) Pollak, E. In *Theory of Chemical Reaction Dynamics*; Baer, M., Ed.; CRC Press: Boca Raton, 1985; Vol. 43, Chapter 2. (b) Truhlar, D. G.; Isaacson, A. D.; Garrett, B. C. In *Theory of Chemical Reaction Dynamics*; Baer, M. Ed.; CRC Press: Boca Raton, 1985; Vol. 4, Chapter 2.

(24) Steckler R.; Truhlar, D. G.; Garrett, B. C. *J. Chem. Phys.* **1986**, *84*, 6712.

(25) Frost, R. J.; Smith, I. W. M. *Chem. Phys.* **1987**, *117*, 389.

(26) Zhang, J. Z. H.; Zhang, Y.; Kouri, D. J., Garrett, B. C.; Haug, K.; Schwenke, D. W.; Truhlar, D. G. *Faraday Discuss. Chem. Soc.* **1987**, *84*, 371.

(27) Agmon, N. *Chem. Phys.* **1983**, *76*, 203.

(28) (a) Natanson, G. A. *Mol. Phys.* **1982**, *46*, 481. (b) Natanson, G. A. *Chem. Phys. Lett.* **1991**, *178*, 49. (c) Ishida, K.; Morokuma, K.; Komornicki, A. *J. Chem. Phys.* **1977**, *66*, 2153. Schmidt, M. W.; Gordon, M. S.; Dupuis, M. *J. Am. Chem. Soc.* **1985**, *107*, 2585. Garrett, B. C.; Redmon, M. J.; Steckler, R.; Truhlar, D. G.; Baldridge, K. K.; Bartol, D.; Schmidt, M. W.; Gordon, M. S. *J. Phys. Chem.* **1988**, *92*, 1476. Baldridge, K. K.; Gordon, M. S.; Steckler, R.; Truhlar, D. G. *J. Phys. Chem.* **1989**, *93*, 5107. Gonzalez, C.; Schlegel, H. B. *J. Phys. Chem.* **1990**, *94*, 5523.

(29) Pollak, E. *J. Chem. Phys.* **1981**, *74*, 5586.

(30) Persky, A.; Broida, M. *J. Chem. Phys.* **1984**, *81*, 4352.

(31) (a) Johnson, B. R.; Winter, N. W. *J. Chem. Phys.* **1977**, *66*, 4116. (b) Song, J.-B.; Gislason, E. A. *Chem. Phys.* **1996**, *202*, 1.

(32) Wilson, E. B., Jr.; Decius, J. C.; Cross, P. C. *Molecular Vibrations: The Theory of Infrared and Raman Vibrational Spectra*; McGraw-Hill: New York, 1955.

(33) Pollak, E.; Wyatt, R. E. *J. Chem. Phys.* **1983**, *78*, 4464.

(34) Smith, I. W. M. *Kinetics and Dynamics of Elementary Gas Reactions*; Butterworth: London, 1980; pp 113.